




Communication

Hydrogen Bonding Directed Self-Assembly of a Binuclear Ag(I) Metallacycle into a 1D Supramolecular Polymer

Anna Brzechwa-Chodzyńska^{1,2}, Mateusz Gołdyn², Anna Walczak^{1,2} , Jack M. Harrowfield³ 
and Artur R. Stefankiewicz^{1,2,*} 

¹ Center for Advanced Technologies, Uniwersytetu Poznańskiego 10, 61-614 Poznań, Poland; anna.brzechwa@amu.edu.pl (A.B.-C.); anna.jenczak@amu.edu.pl (A.W.)

² Faculty of Chemistry, Adam Mickiewicz University, Uniwersytetu Poznańskiego 8, 61-614 Poznań, Poland; mateusz.goldyn@amu.edu.pl

³ Institut de Science et d'Ingénierie Supramoléculaires, Université de Strasbourg, 8 Allée Gaspard Monge, 67083 Strasbourg, France; harrowfield@unistra.fr

* Correspondence: ars@amu.edu.pl

Abstract: An Ag(I) metallacycle obtained unexpectedly during the preparation of Pd(II) complexes of the bifunctional ligand 5-([2,2'-bipyridin]-5-yl)pyrimidine-2-amine (L) has been characterized using X-ray structure determination as a binuclear, metallacyclic species [Ag₂L₂](SbF₆)₂, where both the bipyridine and pyrimidine-N donors of L are involved in coordination to the metal. The full coordination environment of the Ag(I) defines a case of highly irregular 4-coordination. In the crystal, the Ag-metallacycles assemble into one-dimensional supramolecular metalladynamers linked together by hydrogen-bonding interactions.

Keywords: supramolecular chemistry; metalladynamers; H-bond polymers; metallacycles



Citation: Brzechwa-Chodzyńska, A.; Gołdyn, M.; Walczak, A.; Harrowfield, J.M.; Stefankiewicz, A.R. Hydrogen Bonding Directed Self-Assembly of a Binuclear Ag(I) Metallacycle into a 1D Supramolecular Polymer. *Molecules* **2021**, *26*, 5719. <https://doi.org/10.3390/molecules26185719>

Academic Editors: Marek Chmielewski, Patryk Niedbala and Maciej Majdecki

Received: 30 August 2021

Accepted: 16 September 2021

Published: 21 September 2021

Publisher's Note: MDPI stays neutral with regard to jurisdictional claims in published maps and institutional affiliations.



Copyright: © 2021 by the authors. Licensee MDPI, Basel, Switzerland. This article is an open access article distributed under the terms and conditions of the Creative Commons Attribution (CC BY) license (<https://creativecommons.org/licenses/by/4.0/>).

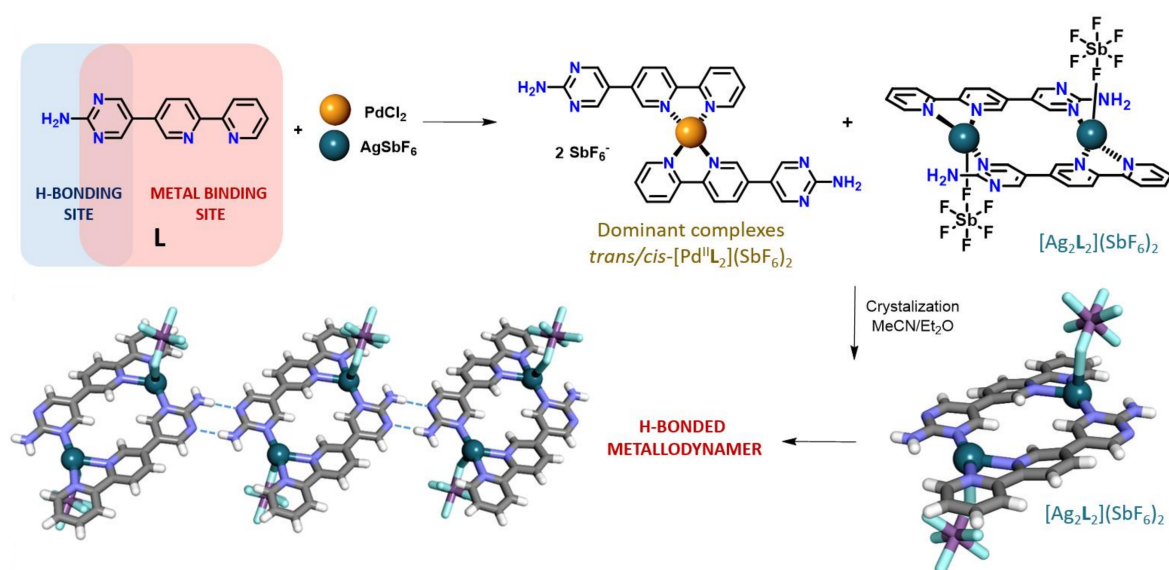
1. Introduction

In the last three decades, a great deal of effort has been devoted to the preparation and further investigation of metallosupramolecular assemblies in the solid state, because they not only extend the range of new structures, which can be designed to possess particular physical and chemical properties but often lead to unexpected applications of such materials [1–3]. In this context, the control of the self-assembly process between labile metal ions and multidentate ligands is a key objective in the development of new metallosupramolecular materials based on the simultaneous use of distinct dynamic linkages [4–6]. Clearly, this process is related to a variety of factors, such as the number, type, and spatial disposition of the binding sites of ligands; the stereoelectronic preferences of metal ions; the solvent used; and the nature of counter ions. [7,8]. The combination of all of these factors leads to numerous metallosupramolecular complexes with various structural topologies and fascinating physicochemical properties [9–15].

Among the various types of supramolecular linkages employed in the generation of complex assemblies, coordination and hydrogen bonds are the most widely employed [16–21]. It is worth noting that despite the incredible progress made in this area of chemistry in recent years, the simultaneous application of both these bonds for the generation of topologically non-trivial supramolecular architectures remains challenging, especially with the use of highly labile metal ions, such as Ag(I) [22–26]. In fact, little attention has been paid to the generation of supramolecular assemblies produced by means of simultaneous hydrogen and coordination bonding with Ag(I) as their metal centers [27–29]. Ag(I) is an interesting metal, with several coordination geometries having been described, such as linear [30], T-shaped [31], trigonal [32], distorted tetrahedral [33], and octahedral geometries [34], and each particular geometry is usually a consequence of the coordination properties of the ligands [35]. In this context, the application of this labile metal ion with a

ligand containing two distinct chelating groups—i.e., pyrimidine and bipyridine—with an additional functional moiety promoting hydrogen bonds remains unexplored.

The bifunctional ligand 5-([2,2'-bipyridin]-5-yl)pyrimidin-2-amine, **L** (Scheme 1), contains both a strong chelation site of the 2,2'-bipyridine type and a strong H-bond acceptor-donor (ADDA) site, a combination anticipated to be of particular utility in the supramolecular chemistry of metal ion complexes. We have shown that with the octahedral metal ion Fe(II) [36], it is possible to isolate both the *meridional* and *facial* forms of its tris(ligand) complexes, in which only the bipyridine site is directly bound to the metal and the aminopyrimidine unit is free to become involved in supramolecular interactions which differ greatly for the two isomers. In contemplating extension of this work to metal ions with different coordination preferences, our first choice was that of a square-planar Pd(II), one of the most versatile and widely used sources of efficient metallocatalysts [37–41]. Again (Scheme 1), it was expected that two isomers, here *cis* and *trans*, might form and that fractional crystallization might be required in their separation. In the event, fractional crystallization of the product mixture obtained by reacting Pd(SbF₆)₂, obtained in situ by reacting PdCl₂ with AgSbF₆ in aqueous acetonitrile, with **L** did produce two distinct materials, the first a poorly crystalline mixture of the Pd(II) complexes and the second being the unexpected Ag(I)-based metallacycle, [Ag₂L₂](SbF₆)₂. We have also found that isolated Ag(I) complex, self-assembles in the solid state and forms extended 1D supramolecular polymer, consisting of macrocyclic monomers linked together by means of H-bonding interactions.



Scheme 1. Anticipated synthesis of the *cis* and *trans* isomers of [Pd^{II}L₂](SbF₆)₂ accompanied by the inadvertent formation of [Ag₂L₂](SbF₆)₂.

2. Results

While the reaction of Pd(SbF₆)₂ with the ligand **L**, 5-([2',2''-bipyridin]-5'-yl) pyrimidin-2-amine does indeed give rise to isomeric forms of the complex [PdL₂]²⁺ (Scheme 1; work to be reported elsewhere), on the very first occasion that it was conducted an apparent excess (0.1 equiv.) of AgSbF₆ in the reaction mixture led to these isomers being produced along with the Ag(I) complex.

Thus, a suspension of the ligand in CH₃CN was mixed at room temperature with a CH₃CN:H₂O (1:1) solution of Pd(SbF₆)₂, generated in situ from PdCl₂ and AgSbF₆, and stirred until a clear yellow solution had formed. As the color appeared consistent with the binding of the bipyridine unit to Pd(II), ESI-MS analysis (Supplementary Figures S3 and S4 in ESI) showed a dominant peak for the ion [Pd^{II}L₂(SbF₆)]⁺ the solution was evaporated to dryness and the residue redissolved in pure CH₃CN. A vapor diffusion of diethylether into this solution with the intention of isolating the [Pd^{II}L₂](SbF₆)₂ presumed to be present

initially provided poorly crystalline material, but on removing this and allowing the supernatant to evaporate slowly, small, pale-yellow crystals were obtained. These proved to be almost completely insoluble in any solvent, indicating that the species originally formed in CH₃CN was no longer present. The exact nature of this material was established by X-ray structure determination (and subsequent chemistry). Thus, the isolated crystalline complex proved not to be a chelate complex of Pd(II) but a diargentacycle, bis[5-(2',2''-bipyridinyl)pyrimidin-2-amine]disilver(I) bis(hexafluoroantimonate), [Ag₂L₂](SbF₆)₂, involving Ag(I) in a four-coordinate environment provided by not only the two N-donors of the bipyridine unit but also by one pyrimidine-N and one fluorine of [SbF₆][−] (Figure 1a). The crystal and structure refinement data for this complex are given in Table 1. Unlike the Fe(II) complexes of L, the ligand here acts as a triple N-donor by bridging the two Ag(I) centers. The binuclear complex unit is centrosymmetric, with Ag–N bond lengths which vary significantly—namely, Ag1–N3 2.151(10); Ag1–N4 2.385(10); and Ag1–N5 2.217(10) Å—covering a range similar to that of the known [Ag(2,2'-bipyridine)₂]⁺ species [42]. Within the diargentacycle unit, the Ag⋯Ag separation is 7.879(2) Å and while there is a shorter separation of 4.862(2) Å between Ag centers in adjacent diargentacycles (Figure 1b), both clearly indicate a lack of metal-metal interactions.

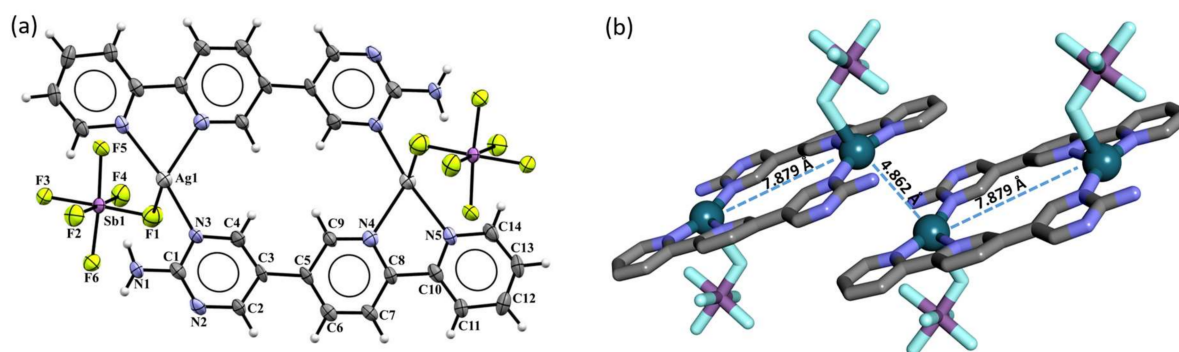


Figure 1. (a) ORTEP representation of the stoichiometric unit of [Ag₂L₂](SbF₆)₂ (Ag1–N3 2.151(10); Ag1–N4 2.385(10); and Ag1–N5 2.217(10) Å). Atom numbering is given for the asymmetric unit and the displacement probability ellipsoids are shown at the 50% level, (b) Ag⋯Ag separations within one molecule and between adjacent molecules (H-atoms have been omitted for clarity).

Table 1. Crystal and structure refinement data for [Ag₂L₂](SbF₆)₂.

Chemical Formula	C ₂₈ H ₂₂ F ₁₂ N ₁₀ Ag ₂ Sb ₂
Formula weight/g mol ^{−1}	1182.85
Crystal system	monoclinic
Space group	P2 ₁ /n
a/Å	8.7047(2)
b/Å	10.6721(3)
c/Å	18.4607(5)
α/°	90
β/°	103.255(3)
γ/°	90
V/Å ³	1669.26(8)
Z	2
2θ Range/°	9.638–151.172
	h = −10→10
Index ranges	k = 0→12
	l = 0→23
D _x /g cm ^{−3}	2.359
μ/mm ^{−1}	22.961
Temperature/K	100.0(1)
F(000)	1128.0

Table 1. Cont.

Chemical Formula	$C_{28}H_{22}F_{12}N_{10}Ag_2Sb_2$
Reflections collected	3325
Independent reflections	3325
Reflections with $I > 2\sigma(I)$	2955
R_{int}	merged
Number of refined parameters	246
$R[F^2 > 2\sigma(F^2)]$	0.065
$wR(F^2)$	0.191

Silver(I) is somewhat notorious for its variety of coordination numbers and the irregularity of its coordination sphere [43], and the present complex provides further examples. The coordination geometry is very irregular, with the Ag displaced only slightly (0.209 (2) Å) from the plane of the three N-donors, but the bond angles N3-Ag1-N4 120.9°, N3-Ag1-N5 161.8°, and N4-Ag1-N5 72.5° are very far from those for a trigonal environment. The displacement of Ag is clearly towards the fourth donor atom provided by the $[SbF_6]^-$. One NH atom does lie close to what might be considered a coordination site, which would give the Ag a nearly square-planar N_3H environment, but the estimated $Ag \cdots H$ distance of 2.7 Å seems too long for any agostic interaction [44] to be significant.

While there are different forms of coordination of the ligand **L** to Ag(I) and Fe(II), the complexes of $[Ag_2L_2](SbF_6)_2$ and *mer*- $[Fe^II L_3](BF_4)_2 \cdot 9H_2O$ [36] in the solid state share a common mode of interaction involving the amino-pyrimidine units, where just half of the capacity of one unit, as ADDA H-bonding entities, is used in the formation of single-strand polymers (Figure 2).

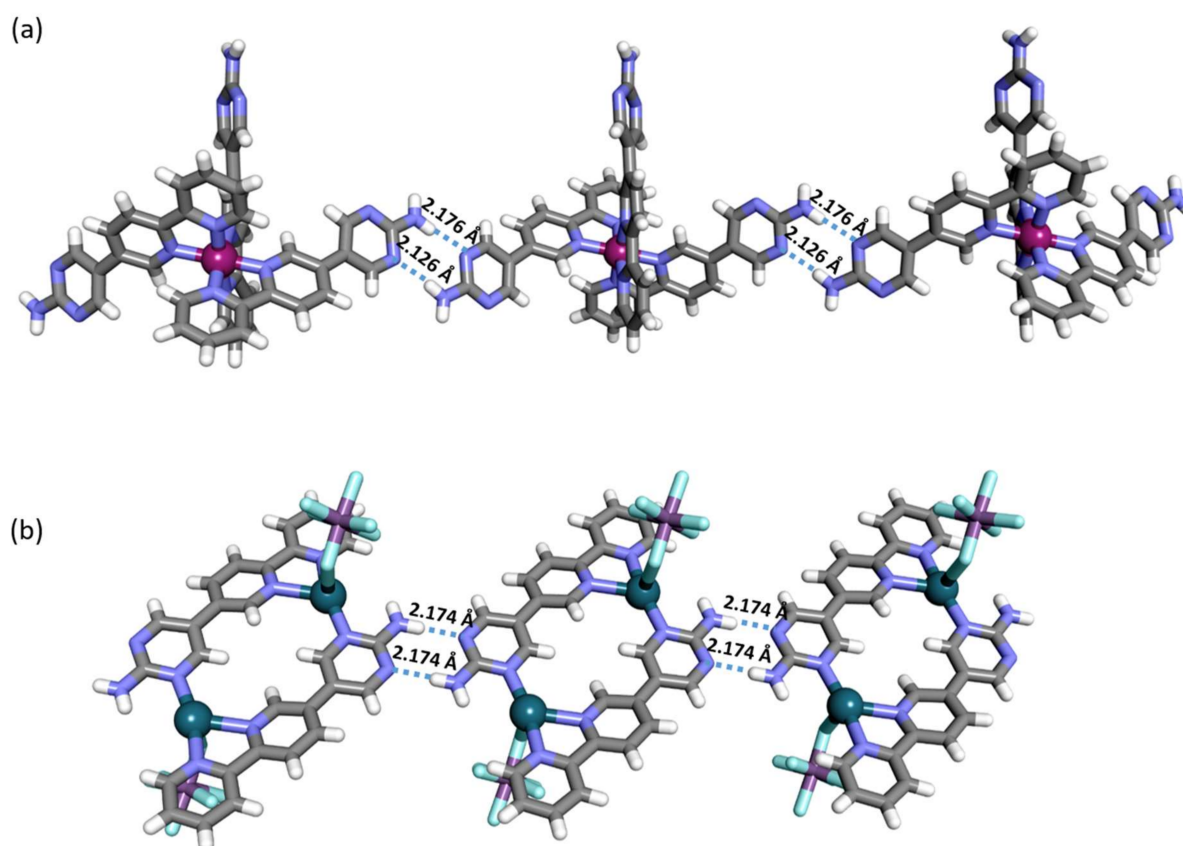


Figure 2. (a) Portion of the polymer formed by the $[Fe^II L_3](BF_4)_2 \cdot 9H_2O$, (b) portion of the polymer formed by the $[Ag_2 L_2](SbF_6)_2$.

In the silver complex structure, two independent single-stranded H-bond polymer units can be observed, running along the [110] and [1-10] crystallographic directions (Figure 3). These strands are cross linked by the multiple F...HN and F...HC interactions of the $[\text{SbF}_6]^-$ units in addition to their coordination to Ag(I), all evident on the Hirshfeld surface [45] (calculated using CrystalExplorer) [46] of the anion formally present. A full listing of the H-bonding interactions within the structure of $[\text{Ag}_2\text{L}_2](\text{SbF}_6)_2$ is given in Table 2. Un-like the structure of $\text{mer-}[\text{Fe}^{\text{II}}\text{L}_3](\text{BF}_4)_2 \cdot 9\text{H}_2\text{O}$, that of $[\text{Ag}_2\text{L}_2](\text{SbF}_6)_2$ shows no evidence of significant apparent void space (Figure S6).

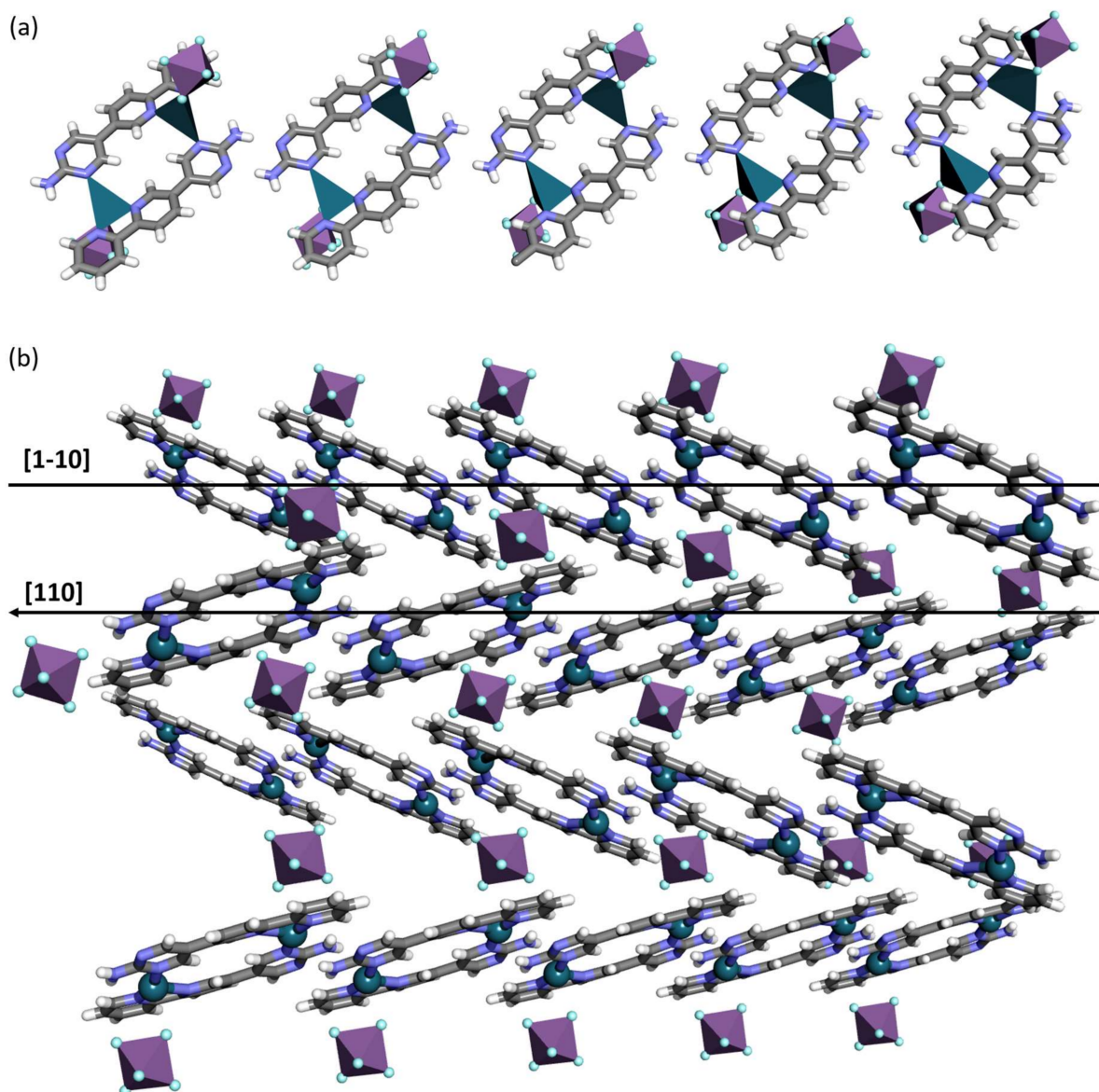


Figure 3. (a) Single-stranded H-bonded polymer system; (b) the lattice, viewed along the [100] direction, showing adjacent non-covalently linked polymer systems running along the [110] and [1-10] directions.

Table 2. Hydrogen bond geometry in $[\text{Ag}_2\text{L}_2](\text{SbF}_6)_2$.

$D-H \cdots A$	$D-H$ [Å]	$H \cdots A$ [Å]	$D \cdots A$ [Å]	$D-H \cdots A$ [°]
C9—H9...F3 ⁱⁱ	0.95	2.69	3.558 (14)	152
N1—H1A...N2 ⁱⁱⁱ	0.81	2.17	2.954 (13)	163
N1—H1B...F4 ^{iv}	0.88	2.37	2.914 (13)	120
C12—H12...F5 ^{viii}	0.95	2.84	3.452 (14)	123

Table 2. Cont.

<i>D</i> —H... <i>A</i>	<i>D</i> —H [Å]	H... <i>A</i> [Å]	<i>D</i> ... <i>A</i> [Å]	<i>D</i> —H... <i>A</i> [°]
C11—H11...F6 ^{vii}	0.95	2.56	3.147 (14)	120
C6—H6...F5 ^v	0.95	2.64	3.264 (12)	124
C6—H6...F3 ^v	0.95	2.45	3.364 (13)	162
C13—H13...F6 ^{vi}	0.95	2.72	3.307 (15)	121
C14—H14...F6 ^{vi}	0.95	2.58	3.250 (13)	128
C14—H14...F4 ^{vi}	0.95	2.57	3.507 (15)	170
C2—H2...F5 ^v	0.95	2.47	3.301 (13)	146

Symmetry codes: (ii) $x - 1/2, -y + 3/2, z - 1/2$; (iii) $-x + 1, -y + 2, -z + 1$; (iv) $-x + 1/2, y + 1/2, -z + 3/2$; (v) $x + 1/2, -y + 3/2, z - 1/2$; (vi) $x - 1/2, -y + 1/2, z - 1/2$; (vii) $-x + 1, -y + 1, -z + 1$; (viii) $x + 1/2, -y + 1/2, z - 1/2$.

3. Materials and Methods

3.1. General Methods

Basic chemicals and solvents were purchased from commercial sources and were used without further purification. The ¹H NMR spectra were acquired on Bruker Fourier 300 or 600 spectrometers equipped with a ¹H 5 mm probe and referenced to the solvent residual peaks (CD₃CN/D₂O, DMSO-*d*₆). NMR solvents were purchased from Deutero GmbH (Kastellaun, Germany) and used as received. The ESI-MS spectra were recorded on a Bruker Impact HD Q-TOF spectrometer in the positive ion mode. Powder X-ray diffraction patterns (PXRD) were recorded on a BRUKER D8-Focus Bragg–Brentano X-ray powder diffractometer equipped with a Cu sealed tube ($\lambda = 1.54178$ Å) at room temperature. Experimental and calculated powder patterns from the crystal structures were analyzed using the Kdif software [47].

3.2. Details of the Crystal Structure Solution and Refinement

Single-crystal diffraction data for the [Ag₂L₂](SbF₆)₂ were collected on a Rigaku XtaLAB Synergy-R diffractometer with a rotating anode using a CuK α radiation source ($\lambda = 1.54184$ Å). The low temperature was achieved using the Cryostream cooling system. Data collection and data reduction were performed using the CrysAlis PRO software [48]. The structure was solved and refined using SHELXT-2015 (intrinsic phasing method) and SHELXL-2015 (least-squares method), respectively [49,50]. Olex2 provided the support for the full structural analysis of the complex [51]. A twin matrix $-1\ 0\ 0\ 0\ -1\ 0\ 0.973\ 0\ 1$, which corresponds to a 180° rotation about the [001] reciprocal lattice direction, was also determined using the Olex2 software. The measured crystal was identified as a non-merohedral twin. The refinement process was performed using the diffraction data written in the HKLF 5 format. The BASF parameter was refined at 0.0964(17). All non-hydrogen atoms were refined with anisotropic displacement parameters. All hydrogen atoms were positioned geometrically in their calculated positions and refined using the riding hydrogen model.

3.3. Experimental Data for the Complex [Pd^{II}L₂](SbF₆)₂

The complex (bis[5-(2,2'-bipyridin)-5-yl]pyrimidin-2-amine)-palladium(I) bis(hexafluoroantimonate)-[Pd^{II}L₂](SbF₆)₂ was prepared using simple procedures, analogous to those used to obtain the iron(II) complex [36]. A suspension of the ligand L (25.0 mg, 0.1 mmol, 2.00 equiv.) in MeCN (5 mL), was stirred for 10 min at room temperature.

Then, the Pd(SbF₆)₂ salt was prepared by mixing PdCl₂ (0.05 mmol, 1 equivalent) dissolved in 2.5 mL of MeCN, and AgSbF₆ (0.105 mmol, 2.1 equivalent) dissolved in 2.5 mL of H₂O. The mixture was stirred for 15 min at room temperature and then filtered through a syringe filter. This freshly generated Pd(SbF₆)₂ (0.05 mmol, 1.00 equivalent) was added to the ligand in the CH₃CN and the resulting clear yellow solution was stirred at room temperature for 30 min. The solution was then evaporated to dryness under reduced pressure and the residue redissolved in MeCN (1 mL). The addition of diethylether (10 mL)

produced a pale-yellow precipitate, which was collected by centrifugation, washed with diethyl ether (20 mL) and dried in vacuo, providing a yellow solid (20 mg, yield 34%). HR-MS (TOF-MS) calculated for $C_{28}H_{22}F_6N_{10}PdSb^+ [M-(SbF_6)]^+$: $m/z = 841.0011$; observed: $m/z = 841.0090$.

3.4. Experimental Data for the Complex $[Ag_2L_2](SbF_6)_2$

After dissolving the residue from the initial reaction mixture in acetonitrile and fractional crystallization, first by the diffusion of diethyl ether into acetonitrile (giving microcrystals collected by filtration as described above) and then by the slow evaporation of the filtrate, light yellow crystals of the $[Ag_2L_2](SbF_6)_2$ complex were obtained with a 5% yield of the reaction. Elem. Anal. calculated for $C_{28}H_{22}F_{12}N_{10}Ag_2Sb_2 \cdot 7H_2O$: C, 25.64; H, 2.77; N, 10.68. Found: C, 25.67; H, 1.65; N, 10.60 (%). No satisfactory elemental analysis was obtained due to its hygroscopic property.

4. Conclusions

In this report, we have described the synthesis and structural analysis of a new binuclear macrocycle in which labile Ag(I) ions are coordinated using a very unique chelating system based on functionalized pyrimidine, bipyridine, and fluorine atoms derived from SbF_6^- counter ions. Moreover, the generated macrocyclic systems undergo further interaction in the solid state, creating a one-dimensional supramolecular polymer in which individual units are connected with each other by hydrogen bonding interactions. Comparison of the now known structures of the Fe(II) and Ag(I) complexes of 5-([2,2'-bipyridin]-5-yl)pyrimidin-2-amine showed that the coordination mode of this ligand is not predictable and clearly can vary considerably with the metal ion chosen. Nonetheless, in both of these known cases the bound ligand retained the capacity to act as an H-bond donor-acceptor, indicating that the solid state supramolecular chemistry has significant prospects for further development, especially with regard to catalytic applications such as those envisaged for the Pd(II) complexes initially targeted in the present work [52,53].

Supplementary Materials: The following are available online, Figure S1: 1H NMR spectrum (600 MHz) of the reaction mixture $[Pd^{II}L_2](SbF_6)_2$. Figure S2: 1H NMR spectrum (600 MHz) of comparisons free ligand and isolated material (see Figure S1) in deuterated MeCN and DMSO. Figure S3: HR-TOF-ESI-MS analysis of the reaction mixture $[Pd^{II}L_2](SbF_6)_2$. Figure S4: HR-TOF-ESI-MS analysis of the reaction mixture $[Pd^{II}L_2](SbF_6)_2$. Figure S5: Kinetic 1H NMR spectrum (600 MHz, CD_3CN) of the reaction mixture $[Pd^{II}L_2](SbF_6)_2$. Figure S6: Void analysis of complex $[Ag_2L_2](SbF_6)_2$, and complex $[Fe^{II}L_3](BF_4)_2 \cdot 9H_2O$ performed with mercury.

Author Contributions: A.B.-C., A.W., J.M.H., and A.R.S. conceived and designed the experiments; A.W., A.B.-C., and M.G. performed the synthetic work and analyzed the data; J.M.H. and A.R.S. made crucial revisions of the manuscript. All authors have read and agreed to the published version of the manuscript.

Funding: A.R.S. thanks the National Science Centre (grant SONATA BIS 2018/30/E/ST5/00032) for financial support. A.B.C and M.G want to acknowledge financial support from the European Union through grant no. POWR.03.02.00-00-I026/16 co-financed by the European Union through the European Social Fund under the Operational Program Knowledge Education Development. A.W. is supported by the Foundation for Polish Science (FNP).

Institutional Review Board Statement: Not applicable.

Informed Consent Statement: Not applicable.

Data Availability Statement: The crystal data for $[Ag_2L_2](SbF_6)_2$ have been deposited in the Cambridge Crystallographic Data Centre (CCDC) with deposition number CCDC 2065082. These data can be obtained free of charge via www.ccdc.cam.ac.uk/data_request/cif, or by emailing data_request@ccdc.cam.ac.uk, or by contacting The Cambridge Crystallographic Data Centre, 12, Union Road, Cambridge CB2 1EZ, UK.

Acknowledgments: The authors would like to thank Agnieszka Kiliszek and Martyna Pluta from the Institute of Bioorganic Chemistry of the Polish Academy of Sciences in Poznań for their help and for providing the XtaLAB Synergy-R diffractometer for crystal data collection.

Conflicts of Interest: The authors declare no conflict of interest. The funders had no role in the design of the study; in the collection, analysis, or interpretation of data; in the writing of the manuscript; or in the decision to publish the results.

References

1. Desiraju, G.R. Supramolecular Synthons in Crystal Engineering—A New Organic Synthesis. *Angew. Chem. Int. Ed. Engl.* **1995**, *34*, 2311–2327. [[CrossRef](#)]
2. Kurth, D.G. Metallo-supramolecular modules as a paradigm for materials science. *Sci. Technol. Adv. Mater.* **2008**, *9*, 014103. [[CrossRef](#)]
3. Amouri, H.; Desmarests, C.; Moussa, J. Confined Nanospaces in Metallogages: Guest Molecules, Weakly Encapsulated Anions, and Catalyst Sequestration. *Chem. Rev.* **2012**, *112*, 2015–2041. [[CrossRef](#)]
4. Ahmadi, M.; Seiffert, S. Coordination Geometry Preference Regulates the Structure and Dynamics of Metallo-Supramolecular Polymer Networks. *Macromolecules* **2021**, *54*, 1388–1400. [[CrossRef](#)]
5. Sun, W.Y.; Yoshizawa, M.; Kusukawa, T.; Fujita, M. Multicomponent metal–ligand self-assembly. *Curr. Opin. Chem. Biol.* **2002**, *6*, 757–764. [[CrossRef](#)]
6. Ward, M.D.; Raithby, P.R. Functional behaviour from controlled self-assembly: Challenges and prospects. *Chem. Soc. Rev.* **2013**, *42*, 1619–1636. [[CrossRef](#)]
7. Chakrabarty, R.; Mukherjee, P.S.; Stang, P.J. Supramolecular Coordination: Self-Assembly of Finite Two- and Three-Dimensional Ensembles. *Chem. Rev.* **2011**, *111*, 6810–6918. [[CrossRef](#)] [[PubMed](#)]
8. Smulders, M.M.; Riddell, I.A.; Browne, C.; Nitschke, J.R. Building on architectural principles for three-dimensional metallo-supramolecular construction. *Chem. Soc. Rev.* **2013**, *42*, 1728–1754. [[CrossRef](#)] [[PubMed](#)]
9. Whittell, G.R.; Hager, M.D.; Schubert, U.S.; Manners, I. Functional soft materials from metallopolymers and metallosupramolecular polymers. *Nat. Mater.* **2011**, *10*, 176–188. [[CrossRef](#)]
10. Bocian, A.; Drożdż, W.; Szymańska, M.; Lewandowski, J.; Fik-Jaskółka, M.; Gorczyński, A.; Patroniak, V.; Stefankiewicz, A.R. Complex-decorated surfactant-encapsulated clusters (CD-SECs) as novel multidynamic hybrid materials. *Nanoscale* **2020**, *12*, 4743–4750. [[CrossRef](#)]
11. Drożdż, W.; Bessin, Y.; Gervais, V.; Cao, X.Y.; Lehn, J.M.; Stefankiewicz, A.R.; Ulrich, S. Switching Multivalent DNA Complexation using Metal-Controlled Cationic Supramolecular Self-Assemblies. *Chem.-A Eur. J.* **2018**, *24*, 1518–1521. [[CrossRef](#)]
12. Brzechwa-Chodzyńska, A.; Drożdż, W.; Harrowfield, J.; Stefankiewicz, A.R. Fluorescent sensors: A bright future for cages. *Coord. Chem. Rev.* **2021**, *434*, 213820. [[CrossRef](#)]
13. Qin, H.; Zhao, C.; Sun, Y.; Ren, J.; Qu, X. Metallo-supramolecular Complexes Enantioselectively Eradicate Cancer Stem Cells in Vivo. *J. Am. Chem. Soc.* **2017**, *139*, 16201–16209. [[CrossRef](#)] [[PubMed](#)]
14. Zhang, Y.; Ali, B.; Wu, J.; Guo, M.; Yu, Y.; Liu, Z.; Tang, J. Construction of Metallosupramolecular Coordination Complexes: From Lanthanide Helicates to Octahedral Cages Showing Single-Molecule Magnet Behavior. *Inorg. Chem.* **2019**, *58*, 3167–3174. [[CrossRef](#)] [[PubMed](#)]
15. Zhang, C.; Patil, R.S.; Atwood, J.L. Chapter Five—Metallosupramolecular Complexes Based on Pyrogallol[4]arenes. In *Advances in Inorganic Chemistry*; van Eldik, R., Puchta, R., Eds.; Academic Press: Cambridge, MA, USA, 2018; Volume 71, pp. 247–276.
16. Hawes, C.S. Coordination sphere hydrogen bonding as a structural element in metal–organic Frameworks. *Dalton Trans.* **2021**, *50*, 6034–6049. [[CrossRef](#)] [[PubMed](#)]
17. Čonková, M.; Drożdż, W.; Miłosz, Z.; Cecot, P.; Harrowfield, J.; Lewandowski, M.; Stefankiewicz, A.R. Influencing prototropy by metal ion coordination: Supramolecular transformation of a dynamer into a Zn-based toroidal species. *J. Mater. Chem. C* **2021**, *9*, 3065–3069. [[CrossRef](#)]
18. Kołodziejski, M.; Brock, A.J.; Kurpik, G.; Walczak, A.; Li, F.; Clegg, J.K.; Stefankiewicz, A.R. Charge Neutral [Cu₂L₂] and [Pd₂L₂] Metalloclusters: Self-Assembly, Aggregation, and Catalysis. *Inorg. Chem.* **2021**, *60*, 9673–9679. [[CrossRef](#)]
19. Beatty, A.M. Hydrogen bonded networks of coordination complexes. *CrystEngComm* **2001**, *3*, 243–255. [[CrossRef](#)]
20. Shi, Q.; Zhou, X.; Yuan, W.; Su, X.; Neniškis, A.; Wei, X.; Taujenis, L.; Snarskis, G.; Ward, J.S.; Rissanen, K.; et al. Selective Formation of S₄- and T-Symmetric Supramolecular Tetrahedral Cages and Helicates in Polar Media Assembled via Cooperative Action of Coordination and Hydrogen Bonds. *J. Am. Chem. Soc.* **2020**, *142*, 3658–3670. [[CrossRef](#)]
21. Therrien, B. Combining Coordination and Hydrogen Bonds to Develop Discrete Supramolecular Metallo-Assemblies. *Chemistry* **2020**, *2*, 565–576. [[CrossRef](#)]
22. Lindoy, L.F.; Park, K.M.; Lee, S.S. Metals, macrocycles and molecular assemblies—Macrocyclic complexes in metallo-supramolecular chemistry. *Chem. Soc. Rev.* **2013**, *42*, 1713–1727. [[CrossRef](#)] [[PubMed](#)]
23. Kurth, D.G.; Higuchi, M. Transition metal ions: Weak links for strong polymers. *Soft Matter* **2006**, *2*, 915–927. [[CrossRef](#)] [[PubMed](#)]
24. Aakeröy, C.B. Supramolecular assembly of low-dimensional silver(I) architectures via amide–amide hydrogen bonds. *Chem. Commun.* **1998**, 1067–1068. [[CrossRef](#)]

25. Chainok, K.; Neville, S.M.; Forsyth, C.M.; Gee, W.J.; Murray, K.S.; Batten, S.R. Supramolecular architecture of silver(I) coordination polymers containing polydentate N-donor ligands. *CrystEngComm* **2012**, *14*, 3717–3726. [CrossRef]
26. Sun, D.; Cao, R.; Sun, Y.; Bi, W.; Li, X.; Wang, Y.; Shi, Q.; Li, X. Novel Silver-Containing Supramolecular Frameworks Constructed by Combination of Coordination Bonds and Supramolecular Interactions. *Inorg. Chem.* **2003**, *42*, 7512–7518. [CrossRef] [PubMed]
27. Chen, C.L.; Kang, B.S.; Su, C.Y. Recent Advances in Supramolecular Design and Assembly of Silver(I) Coordination Polymers. *Aust. J. Chem.* **2006**, *59*, 3–18. [CrossRef]
28. Metherell, A.J.; Ward, M.D. Coordination chemistry of an amine-substituted bis(pyrazolyl)-pyridine ligand: Interaction of a peripheral functional group on a coordination cage with the internal contents of the cavity. *Supramol. Chem.* **2018**, *30*, 822–831. [CrossRef]
29. Kilpin, K.J.; Gower, M.L.; Telfer, S.G.; Jameson, G.B.; Crowley, J.D. Toward the Self-Assembly of Metal-Organic Nanotubes Using Metal-Metal and π -Stacking Interactions: Bis(pyridylethynyl) Silver(I) Metallo-macrocycles and Coordination Polymers. *Inorg. Chem.* **2011**, *50*, 1123–1134. [CrossRef] [PubMed]
30. Yamada, S.; Ishida, T.; Nogami, T. Supramolecular triangular and linear arrays of metal-radical solids using pyrazolato-silver(i) motifs. *Dalton Trans.* **2004**, 898–903. [CrossRef] [PubMed]
31. Yaghi, O.M.; Li, H. T-Shaped Molecular Building Units in the Porous Structure of $\text{Ag}(4,4'\text{-bpy})\cdot\text{NO}_3$. *J. Am. Chem. Soc.* **1996**, *118*, 295–296. [CrossRef]
32. Jimenez, J.; Chakraborty, I.; Del Cid, A.M.; Mascharak, P.K. Five- and Six-Coordinated Silver(I) Complexes Derived from 2,6-(Pyridyl)iminodiadamantanes: Sustained Release of Bioactive Silver toward Bacterial Eradication. *Inorg. Chem.* **2017**, *56*, 4784–4787. [CrossRef]
33. Patra, G.K.; Goldberg, I. Coordination polymers of transition metal ions with polydentate imine ligands. Syntheses, materials characterization, and crystal structures of polymeric complexes of copper(i), silver(i) and zinc(ii). *J. Chem. Soc. Dalton Trans.* **2002**, 1051–1057. [CrossRef]
34. Navarro, J.R.; Salas, J.; Angustias Romero, M. Influence of anions and crystallisation conditions on the solid-state structure of some binuclear silver(I) complexes supported by triazolopyrimidine bridges. *J. Chem. Soc. Dalton Trans.* **1998**, 901–904. [CrossRef]
35. Njogu, E.M.; Omondi, B.; Nyamori, V.O. Review: Multimetallic silver(I)-pyridinyl complexes: Coordination of silver(I) and luminescence. *J. Coord. Chem.* **2015**, *68*, 3389–3431. [CrossRef]
36. Brzechwa-Chodzyńska, A.; Zieliński, M.; Gilski, M.; Harrowfield, J.M.; Stefankiewicz, A.R. Dynamer and Metallodymer Interconversion: An Alternative View to Metal Ion Complexation. *Inorg. Chem.* **2020**, *59*, 8552–8561. [CrossRef]
37. Jana, R.; Pathak, T.P.; Sigman, M.S. Advances in transition metal (Pd, Ni, Fe)-catalyzed cross-coupling reactions using alkyl-organometallics as reaction partners. *Chem. Rev.* **2011**, *111*, 1417–1492. [CrossRef]
38. Molnár, Á. Efficient, Selective, and Recyclable Palladium Catalysts in Carbon–Carbon Coupling Reactions. *Chem. Rev.* **2011**, *111*, 2251–2320. [CrossRef]
39. Fortman, G.C.; Nolan, S.P. N-Heterocyclic carbene (NHC) ligands and palladium in homogeneous cross-coupling catalysis: A perfect union. *Chem. Soc. Rev.* **2011**, *40*, 5151–5169. [CrossRef]
40. Yin, L.; Liebscher, J. Carbon–Carbon Coupling Reactions Catalyzed by Heterogeneous Palladium Catalysts. *Chem. Rev.* **2007**, *107*, 133–173. [CrossRef]
41. Miyaura, N.; Suzuki, A. Palladium-Catalyzed Cross-Coupling Reactions of Organoboron Compounds. *Chem. Rev.* **1995**, *95*, 2457–2483. [CrossRef]
42. Thuéry, P.; Atoini, Y.; Harrowfield, J. 1,2-, 1,3-, and 1,4-Phenylenediacetate Complexes of the Uranyl Ion with Additional Metal Cations and/or Ancillary N-Donor Ligands: Confronting Ligand Geometrical Proclivities. *Cryst. Growth Des.* **2019**, *19*, 6611–6626. [CrossRef]
43. Eckhardt, S.; Brunetto, P.S.; Gagnon, J.; Priebe, M.; Giese, B.; Fromm, K.M. Nanobio Silver: Its Interactions with Peptides and Bacteria, and Its Uses in Medicine. *Chem. Rev.* **2013**, *113*, 4708–4754. [CrossRef] [PubMed]
44. Saßmannshausen, J. Quo Vadis, agostic bonding? *Dalton Trans.* **2012**, *41*, 1919–1923. [CrossRef] [PubMed]
45. Spackman, M.A.; Jayatilaka, D. Hirshfeld surface analysis. *CrystEngComm* **2009**, *11*, 19–32. [CrossRef]
46. Wang, H.; Xiao, H.; Liu, N.; Zhang, B.; Shi, Q. Three New Compounds Derived from Nitrofurantoin: X-ray Structures and Hirshfeld Surface Analyses. *Open J. Inorg. Chem.* **2015**, *5*, 63. [CrossRef]
47. Knížek, K. Institute of Physics ASCR, KDif V3.00a (Kalvados-Software for Crystal Structure and Powder Diffraction). Available online: <https://www.fzu.cz/~knizek/kalvados/index.html> (accessed on 17 September 2021).
48. Diffraction, R.O. *CrysAlisPro Software System*; Rigaku Corporation: Wroclaw, Poland, 2020.
49. Sheldrick, G.M. Crystal structure refinement with SHELXL. *Acta Crystallogr. C* **2015**, *71*, 3–8. [CrossRef]
50. Sheldrick, G.M. SHELXT—Integrated space-group and crystal-structure determination. *Acta Crystallogr. A* **2015**, *71*, 3–8. [CrossRef]
51. Dolomanov, O.V.; Bourhis, L.J.; Gildea, R.J.; Howard, J.A.; Puschmann, H. OLEX2: A complete structure solution, refinement and analysis program. *J. Appl. Crystallogr.* **2009**, *42*, 339–341. [CrossRef]
52. Resnati, G.; Boldyreva, E.; Bombicz, P.; Kawano, M. Supramolecular interactions in the solid state. *IUCr* **2015**, *2*, 675–690. [CrossRef]
53. Desiraju, G.R. Crystal engineering: Solid state supramolecular synthesis. *Curr. Opin. Solid State Mater. Sci.* **1997**, *2*, 451–454. [CrossRef]